High-temperature behavior of infrared conductivity of a $Pr_2NiO_{4+\delta}$ single crystal

B. Rousseau, D. De Sousa Meneses, A. Blin, M. Chabin, and P. Echegut
Centre de Recherches sur les Matériaux à Haute Température - CNRS, 1D avenue de la Recherche Scientifique, 45701 Orléans Cedex 02, France

P. Odier
Laboratoire de Cristallographie - CNRS, 25 Av. des Martyrs, BP 166, 38042 Grenoble Cedex 09, France

F. Gervais
Laboratoire d'Electrodynamique des Matériaux Avancés, UMR 6157 CNRS-CEA, Faculté des Sciences et Techniques, Université François Rabelais, Parc de Grandmont, 37200 Tours, France
(Received 19 April 2004; revised manuscript received 5 April 2005; published 28 September 2005)

The infrared reflectivity spectra of a $Pr_2NiO_{4+\delta}$ single crystal and its high-temperature dependence (300–1300 K) are investigated for light polarized in the basal plane. Fitting with the appropriate model allows one to discriminate localized and itinerant charge carriers. Below 720 K, a thermally activated behavior of mobile species is observed with $E_a \sim 93$ meV consistent with previous dc resistivity measurements. High-temperature behavior is discussed by considering oxygen loss, structural data (x-ray diffraction, neutron diffraction), and existing models developed at lower temperatures.

DOI: 10.1103/PhysRevB.72.104114 PACS number(s): 78.30.−j, 71.38.−k, 78.40.−q

I. INTRODUCTION

Black oxides of the chemical formula $Ln_2MO_{4+\delta}$—where Ln is a lanthanide and M a $3d$ element—are extensively investigated for their remarkable electronic properties such as high-T_c superconductivity for cuprates,[1] colossal magnetoresistance in manganites,[2] and charge ordering for nickelates.[3,4] Many studies of $Ln_2NiO_{4+\delta}$ compounds have been carried out in the usual temperature range, 4–300 K, because these compounds are isostructural with high-T_c superconducting $La_2CuO_{4+\delta}$.[5–8] Early investigations at higher temperatures evidenced a change of the slope of the conductivity versus temperature around 700 K, initially referred to as a semiconductor-metal phase transition,[9–13] and reinterpreted afterwards in terms of a loss of oxygen at high temperature.[14] The high-oxygen mobility of nickelates makes them attractive for cathode in solid oxide fuel cell devices.[15–19] Moreover their high spectral emissivity can be used to produce efficient infrared heaters.[20] Indeed a rough layer of $Pr_2NiO_{4+\delta}$ emits infrared radiation like a black body.[21] These technological potential applications suggest inspection of the underlying physics in the 300–1300 K temperature range currently not often investigated.

In $Pr_2NiO_{4+\delta}$, the oxygen overstoichiometry δ plays a crucial role on its physical and structural properties,[22–29] since insertion of oxygen relaxes the constraints of the undoped distorted compound and creates holes in the NiO_2 planes,[25–27] inducing highly anisotropic behavior.[22,24] $Pr_2NiO_{4+\delta}$ undergoes a structural phase transition from an orthorhombic symmetry (LTO) to a tetragonal one (HTT) at $T \sim 720$ K,[26] accompanied by oxygen loss.[25] This structural transition may be also correlated to the electrical behavior change occurring also at $T \sim 720$ K,[27] the compound behaving as a semiconductor below this temperature.

The *ab* plane infrared reflectivity of a $Pr_2NiO_{4+\delta}$ single crystal, reported at room temperature by Gervais *et al.* in Ref. 22, cannot be described with a Drude term alone since a strong absorption band was found in the mid-infrared range (MIR). The same features have been experimentally observed in the optical spectra of doped nickelate[7,30–38] and isostructural doped cuprate.[36,39–46] For nickelates, the charge carrier density ($\sim 10^{21}$ cm^{-3}) is lower than in the case of conventional metal ($\geqslant 10^{22}$ cm^{-3}) leading to an incomplete screening of polar phonons. As a result, the charge carriers can interact with each other and/or with the lattice, the latter interaction forming polarons.[36] Several authors have applied the polaronic concept to explain the mid-infrared bands on the spectra of nickelates,[31,33,35,36,38] and cuprates.[36,43,45] Other authors have proposed electron transitions connected with localized states,[47] absorptions involving charge transfer from in-plane O $2p$ to the Ni $3d$ state,[7] or more recently fluctuations of stripes above the ordering temperature[34] and localization by disorder, which apply well to the case of polymers.[48] How will such a strongly correlated-hole system behave at higher temperatures? High-temperature infrared reflectivity measurements of a $Pr_2NiO_{4+\delta(T)}$ single crystal are reported here. Experimental data are discussed and compared with the temperature dependence of excess oxygen measured by a thermogravimetric analysis (TGA) of a small fragment cut in the same sample, our goal being to characterize the nature and the role of charge carriers at high temperature.

II. EXPERIMENT

A large single crystal of $Pr_2NiO_{4+\delta(T)}$ ($3 \times 10 \times 5$ mm) was grown by the floating-zone method with a CO_2 laser under ambient atmosphere.[49] After checking its orientation by Laue back reflection, it was cut along the *ab* plane and optically polished. The oxygen excess ($+\delta$) was measured by thermogravimetry (Setaram TAG 24, sensitivity ±1 μg) with a heating rate of 3 K/min up to 1300 K under air atmo-

sphere. The temperature dependence of the reflectivity spectra $R(\omega)$ was obtained for the polarization within the *ab* plane (80 to 5000 cm^{-1}) with a Fourier transform unfrared Bruker 113v spectrometer, following the same heating procedure as the thermogravimetric analysis. The spectrometer and the device used for high-temperature measurements have been described elsewhere.[50] An aluminum mirror is used as the reference and the data acquisition was performed with an instrumental resolution of 4 cm^{-1}.

III. INFRARED DATA ANALYSIS

Infrared reflectivity $R(\omega)$ is related to the complex dielectric function by the Fresnel equation (in normal incidence),

$$R(\omega) = \left| \frac{\sqrt{\tilde{\varepsilon}(\omega)} - 1}{\sqrt{\tilde{\varepsilon}(\omega)} + 1} \right|^2. \tag{1}$$

In many conducting oxides, the following expression of the dielectric response has been used successfully to reproduce their peculiar optical features over several decades of frequencies:[22–24,35,36,38,40,44,45,51]

$$\frac{\tilde{\varepsilon}(\omega)}{\varepsilon_\infty} = \prod_j \left(\frac{\Omega_{jLO}^2 - \omega^2 + i\gamma_{jLo}\omega}{\Omega_{jTO}^2 - \omega^2 + i\gamma_{jTo}\omega} \right) - \frac{\Omega_p^2 + i(\gamma_p - \gamma_o)\omega}{\omega^2 - i\gamma_o\omega}. \tag{2}$$

In Eq. (2), the product term represents the factorized form of the dielectric function introduced by Kurosawa,[52] Ω_{jTO} and Ω_{jLO} being respectively the transverse (TO) and longitudinal (LO) optical frequencies of the jth oscillator and γ_{jTO} and γ_{jLO} the corresponding TO and LO dampings. This function reproduces the phononic response, and is also used to take into account trapped carriers.[36] An extended Drude term is added to describe the response of mobile carriers, the plasma frequency Ω_P being then given by

$$\Omega_p^2 = \frac{N_{Mob} e^2}{m_{Mob}^* \varepsilon_\nu \varepsilon_\infty}, \tag{3}$$

where N_{Mob} is the density of mobile carriers, m_{Mob}^* their effective mass, ε_ν the vacuum dielectric constant, and ε_∞ the high-frequency dielectric constant that includes the electronic contributions. In the second term, γ_0 represents the scattering rate of the mobile carriers at $\omega=0$ and γ_P the damping calculated at $\omega=\Omega_P$. Advantages and drawbacks of this model were also intensively discussed with regard to other models existing in the literature.[36,44,45] The interest of such type of fitting procedure is its ability to discriminate the contributions of trapped and mobile carriers.[36,51] Moreover, by using their respective spectral weights, one can calculate directly the numbers of self-trapped carriers (N_{Loc}) and mobile carriers (N_{Mob}). Thus, the real part of the optical conductivity, $\sigma_{opt}(\omega)$, is given by

$$\sigma_{opt}(\omega) = \mathrm{Re}[\tilde{\sigma}(\omega)] = \omega\varepsilon_\nu \mathrm{Im}[\varepsilon(\omega)]. \tag{4}$$

With Eq. (2), this expression can be rewritten as

$$\sigma_{opt}(\omega) = \sigma_{osc}(\omega) + \sigma_{Mob}(\omega), \tag{5}$$

where $\sigma_{Mob}(\omega)$ is the contribution of the mobile carriers and $\sigma_{osc}(\omega)$ the coupled contribution of the lattice vibrations and the localized carriers. From Eq. (5) and Eq. (2), $\sigma_{Mob}(\omega)$ can be written

$$\sigma_{Mob}(\omega) = \varepsilon_\nu \varepsilon_\infty \frac{\Omega_p^2 \gamma_o}{\omega^2 + \gamma_o^2} + \varepsilon_\nu \omega^2 \frac{(\gamma_p - \gamma_O)}{\omega^2 + \gamma_0^2}. \tag{6}$$

If the resonance of phonons and of the localized carriers lies in different spectral regions, the contribution to the optical conductivity of the self-trapped carriers $\sigma_{Loc}(\omega)$ will be decoupled,

$$\sigma_{Loc}(\omega) \equiv \varepsilon_\infty \varepsilon_\nu \omega_2 \frac{\left[\gamma_{LO_{Loc}}\left(\Omega_{TO_{Loc}}^2 - \omega^2\right) - \gamma_{TO_{Loc}}\left(\Omega_{TO_{Loc}}^2 - \omega^2\right)\right]}{\left(\Omega_{TO_{Loc}}^2 - \omega^2\right) + \gamma_{TO_{Loc}}^2 \omega^2}. \tag{7}$$

The density of localized carriers, N_{Loc}, can then be estimated by

$$N_{Loc} = \frac{2\, m_{Loc}^*}{\pi\, e^2} \int_0^\infty \sigma_{Loc}(\omega) d\omega, \tag{8}$$

where m_{Loc}^* is the hole effective mass. The density of itinerant carriers, N_{Mob} is deduced from the value of the plasma frequency given by Eq. (3) Note that calculations of N_{Loc} and N_{Mob} are dependent upon the hole effective mass that will be estimated in the following discussion.

Another way currently used to obtain the infrared conductivity $\sigma_{opt}(\omega)$, is to apply a Kramers-Kronig inversion of the reflectivity $R(\omega)$, which yields the phase $\theta(\omega)$.[53,54] From $R(\omega)$ and $\theta(\omega)$, the real part of the complex conductivity $\sigma_{opt}(\omega)$ is calculated. For the extrapolations, a Hagens-Rubens formula has been used in the low frequency range and a ω^{-4} extrapolation in the high frequency range.

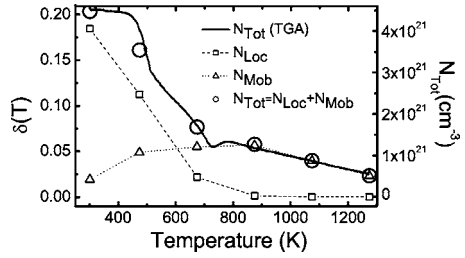

FIG. 1. Variation of the oxygen overstoichiometry $\delta(T)$ of a single crystal of $Pr_2NiO_{4+\delta(T)}$, deduced from the TGA experiment. The corresponding total density of holes in the compound is reported on the right scale. Comparison is between the temperature dependence of the charge carrier density deduced from TGA measurement (dotted curve) and the one calculated from the dielectric function model (symbols). The squares represent the density of localized carriers, N_{Loc}; the triangles, the density of mobile carriers, N_{Mob}; and the circles, the total density, N_{Tot}. N_{Loc} is obtained by applying Eqs. (7) and (8) with a high wave number limit of integration of 50 000 cm^{-1}. The dashed lines are guides for the eyes.

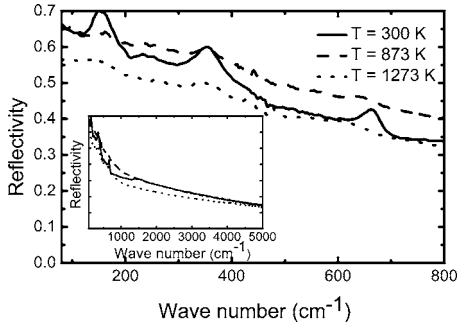

FIG. 2. Temperature dependence of the far infrared reflectivity of a $Pr_2NiO_{4+\delta(T)}$ single crystal for the electric field lying in the *ab* plane. The inset shows the same spectra in the whole experimental spectral range.

IV. RESULTS

A. Thermal weight analysis

The mass temperature dependence of $Pr_2NiO_{4+\delta(T)}$ under airflow is reported in Fig. 1 The initial composition determined by TGA under Ar+5% H_2 flow is $Pr_2NiO_{4.205}$ at $T=300$ K If we assume that, for one oxygen atom injected in the NiO_2 plane, two holes per Ni atom are produced, then the total hole density is $N_{Tot}(T)=8\delta_{(T)}/V_{cell}$, where $V_{cell}=384$ Å^3 is the volume of the cell which contains four formula units.[25] $N_{Tot}(300)$, therefore, is about 4.5×10^{21} cm^{-3} and $N_{Tot}(1300)$ lies around 5.4×10^{20} cm^{-3}. Such a charge carrier density at $T=1300$ K is high enough to certainly play a major role on the optical response.

B. Infrared reflectivity spectra

Figure 2 shows the temperature dependence of the infrared reflectivity spectra within the *ab* plane of $Pr_2NiO_{4.205}$. The data have been recorded at $T=300$, 473, 673, 873, 1073, and 1273 K but only three representative measurements have been plotted (300, 873, and 1273 K) to facilitate the reading of Fig. 2. It can be clearly seen from this figure that the shape of the reflectivity spectra is not deeply affected by the increase of temperature and looks similar to those previously reported for poorly conducting oxides.[7,22,30–33,36,40,43,51]

The infrared spectrum of $Pr_2NiO_{4.205}$ at room temperature is well reproduced by the combination of three phonon peaks, an overdamped oscillator in the mid-infrared range ($\omega_{TO_{Loc}}=3800$ cm^{-1}) and an extended Drude's term ($\Omega_p\sim900$ cm^{-1}) as shows the comparison between the experimental and fitted spectrum reported in Fig. 3 To reproduce satisfactorily the large spectral weight of this band, $\omega_{LO_{Loc}}\sim7200$ cm^{-1} is found, such value being of the same order as the one used to fit the reflectivity spectra of a $Pr_2NiO_{4.22}$ single crystal up to 15 000 cm^{-1}.[54] It is worth noting as the TO-LO splitting acts as the oscillator strength of the conventional Drude-Lorentz model. The parameter values corresponding to our best fit of the room temperature spectra of $Pr_2NiO_{4.205}$ are listed in Table I. To estimate explicitly the spectral weight of the MIR band, we report in Fig. 4 the different contributions to the optical conductivity, by using Eqs. (4)–(7) and it can be seen that the spectral weight assigned to trapped carriers dominates here largely those related to the mobile carriers.

TABLE I. Frequency and damping coefficients which yield the best fit to reflectivity spectra lying in the *ab* plane of a single crystal of $Pr_2NiO_{4.205}$ at $T=300$ K and $T=1273$ K.

T (K)	Ω_{TO} (cm^{-1})	Ω_{LO} (cm^{-1}) Ω_P (cm^{-1})	γ_{TO} (cm^{-1}) γ_0 (cm^{-1})	γ_{LO} (cm^{-1}) γ_P (cm^{-1})
300	144	181	33	88
	341	371	75	112
	671	680	45	41
	3 800	7 200	12 000	12 000
		900	612	755
1 273	147	182	94	174
	366	579	260	308
	642	763	188	379
		998	1 440	4 667

The spectra acquired on the heated sample have been fitted on the basis of the fitting procedure developed for the room temperature spectrum. It can be noted that above 873

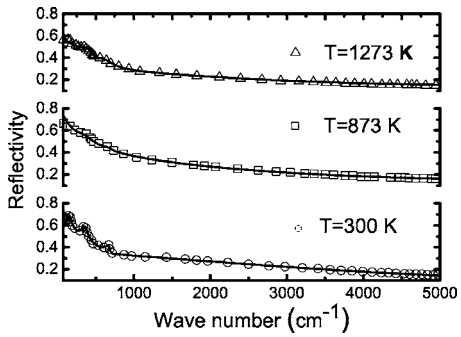

FIG. 3. Comparison between experimental reflectivity (symbols) and best fits using a dielectric function model (solid curves) at $T=300$ K, $T=873$ K, and $T=1273$ K.

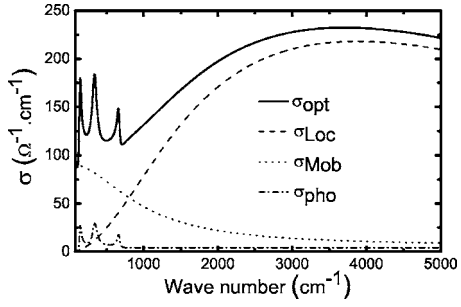

FIG. 4. Detail of the different contributions to the optical conductivity at $T=300$ K obtained with the dielectric function model of (1) phonons (dash-dot line), (2) trapped carriers (dash line), (3) itinerant carriers (dot line), and (4) global response (solid curve). σ_{pho} is obtained by subtracting σ_{Loc} to σ_{osc}, the coupled contributions of localized carrier and lattice vibration.

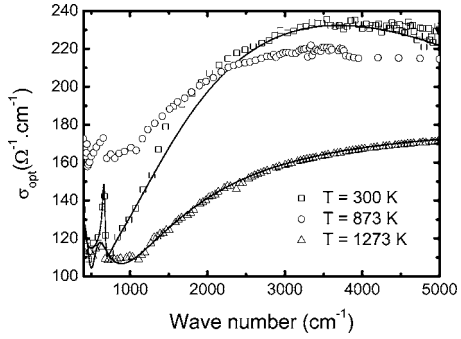

FIG. 5. Temperature dependence of the optical conductivity obtained via the Kramers-Kronig inversions of the infrared (IR) reflectivity spectra. Comparison of the real parts of the optical conductivity performed by Kramers-Kronig inversions (symbol) and from the best fits with the dielectric function model for an *ab* plane of the single crystal of $Pr_2NiO_{4+\delta(T)}$ (solid curve). The fit of the optical conductivity obtained at $T=873$ K is not reported.

K, the contribution of the supplementary oscillator is not required to reproduce the experimental spectra. In Fig. 5 we compare the optical conductivity obtained by using the Kramers-Kronigs inversions with those deduced from the simulation of the complex dielectric function, showing a good agreement between those two procedures. Upon heating, an important loss of spectral weight noted above $T=873$ K, is reported on Fig. 6 that displays the temperature dependence of the optical conductivity of the localized carriers. One can notice that the spectral weight of the MIR band decreases regularly up to $T=873$ K where it becomes rather weak, and that the low frequency onset of the MIR band shifts to lower frequencies when the temperature is rising. This is a well-known behavior since several authors have also reported this evolution on doped La_2NiO_4 compounds, but for lower temperatures.[24,31,34,32] The weakening of the MIR band in the high-temperature range ($T>873$ K) suggests that the mobile carriers are mainly responsible for the optical absorption. Moreover the mobile carriers do not exhibit here a pure Drude-like optical response, since the optical conductivity is not centered at $\omega=0$, but is rather weak at low frequency. As seen from Fig. 2, the mobile carriers do not completely screen the phonons, underlining the fact that they certainly interact with each others or with the lattice. The large variation between the values of γ_0 and

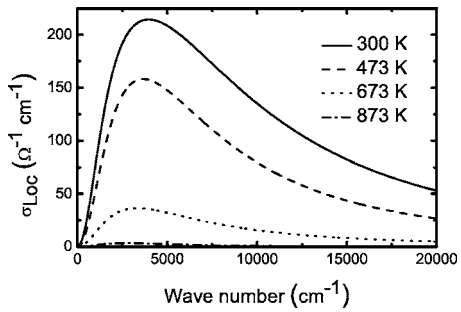

FIG. 6. Temperature dependence of the optical conductivity, due to the contribution of the localized carriers, obtained by applying Eq. (7).

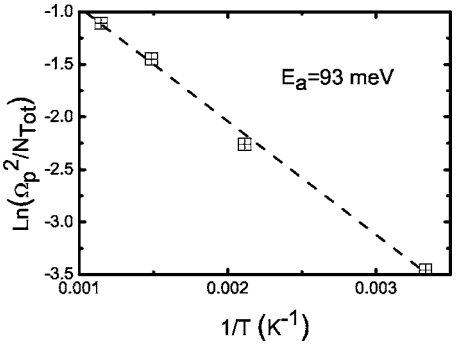

FIG. 7. Temperature dependence of the ratio of the square of the plasma frequency on the total density of carrier obtained from TGA measurements.

γ_P (see Table I) suggests that the mobile carriers rather follow an incoherent diffusion motion.[36,45,51]

By exploiting the temperature dependence of the plasma frequency, we can now provide more precisions on the behavior of the mobile species. increases Ω_P up to a broad maximum attained between 673 K and 873 K ($\sim$1600 cm^{-1}), corresponding to the highest reflectivity level, and then decreases down to 1000 cm^{-1} at 1273 K (see Table I). For $La_{1.84}Sr_{0.16}NiO_{4+\delta}$, Crandles *et al.* have found that Ω_P^2 shows a thermal[14] activated behavior below room temperature,[32] but because of the chemical evolution of our compound (see Sec. IV A), we cannot verify this straightforwardly. However by renormalizing Ω_P^2 with N_{Tot} deduced from the TGA measurement, we show that this ratio remains thermally activated up to $T=873$ K with $E_a\sim93$ meV (see Fig. 7).

It is useful to quantify the temperature dependence of N_{Mob} and N_{Loc}. Since above 720 K N_{Mob} tends towards N_{Tot}, let us assume that $N_{Mob}=N_{Tot}$. One can therefore estimate that $m^*_{Mob}\sim11\ m_e$ by using Eq. (3), the plasma frequency being known. From this effective mass, one can now calculate the value of N_{Mob} below 720 K and consequently those of $N_{Loc}(N_{Loc}=N_{Tot}-N_{Mob})$. We note that N_{Loc} is also consistent with the density of localized carriers obtained by applying Eqs. (7) and (8) and by using $m^*_{Loc}\sim3\ m_e$. Figure 1 summarizes the temperature dependence of N_{Mob} and N_{Loc}, and a good correlation is found between N_{Tot} deduced from oxygen mass loss and $N_{Loc}+N_{Mob}$, both values being issued from the spectroscopic analysis. The large value of m^*_{Mob} is not surprising since similar values were reported by using an infrared spectra analysis: $m^*_{Mob}\sim11\ m_e$ for a $LaNi_{1-x}Fe_xO_3$ solid solution,[55] $m^*_{Mob}\sim10\ m_e$ for doped La_2CuO_4,[40] and $m^*_{Mob}\sim30\ m_e$ for $La_{2-x}Sr_xNiO_4$.[30]

The high-temperature spectroscopic data show evidence of two distinct regimes: the first, noted as regime 1, is governed by the coexistence of localized and itinerant carriers (below $\sim$720 K) and the second (noted as regime 2) is dominated by diffusive itinerant carriers (above $\sim$720 K). Both regimes are consistent with observed from previous dc resistivity measurement experiments on a $Pr_2NiO_{4+\delta}$.[27] For regime 1, the orthorhombic distortion can promote a strong interaction between the charge carriers and the ions of the NiO_2 plans,[58] that suggests the formation of polarons. The

suppression of this chemical pressure at $T=720$ K,[25,27] may be correlated with the decrease of the density of localized carriers. This analysis is also reinforced by previous optical studies at room temperature,[35] which also exhibit absorption mechanisms in the mid-infrared range that can be generated by localized polarons.[24,31,34–36,38,51] Other theoretical and experimental studies,[59–62] previously realized on isostructural cuprate compounds, also underline the polaronic nature of the charge carriers.

We can support such a polaronic approach if we also consider the excellent agreement found between activation energies obtained, respectively, by infrared analysis ($E_a \sim 93$ meV) and by dc measurements ($E_a \sim 95$ meV). It is suggested here that the same microscopic mechanism is involved on both phenomena. Allançon in Ref. 56 showed that the temperature dependence of the static electrical conductivity is well fitted with an adiabatic small polaron hopping's law.[57]

Conversely, structural data[25,26] showing ordered interstitial oxygen in the LTO phase[27] do not plead in favor of an interpretation based on localization by disorder. Moreover, from an optical point of view, the spectroscopic signature of localized carriers does not occur in the far infrared range as is predicted for this concept. Therefore, for regime 1, a polaronic picture allows us to describe the optical and the electrical behavior of the compound.

In regime 2, we have shown that the carriers propagate certainly in the lattice according to an incoherent scattering mechanism. Such a scheme has been proposed by Bassat *et al.* to interpret the linear evolution of the resistivy of a $La_{2-x}NiO_{4+\delta}$ sample upon heating ($T>600$ K),[14] this linear evolution being attributed "to the motion of itinerant holes of short mean-free path in the HTT phase."[63] This kind of motion has been recently proposed by Takenaka *et al.* to interpret the transport properties of a $La_{2-x}Sr_xCuO_4$ single crystal up to $T=1000$ K.[46] Here we propose that a polaronic picture may be used to interpret this regime; a polaronic picture allows us to propose a reasonable interpretation of the whole temperature dependence of the infrared conductivity of $Pr_2NiO_{4+\delta}$.

V. CONCLUSION

In this work, we highlight the strong correlation between the chemical doping $\delta(T)$ of $Pr_2NiO_{4+\delta}$ and its electrical and optical properties. The excess oxygen inserted between the Pr-O layers generates holes in the NiO_2 plane, which interact with the lattice to form polarons consistent with high-temperature infrared spectroscopy and TGA measurements. Mobile and localized polaron contributions have been estimated by combining mass loss analysis with simulation of the infrared reflectivity spectra. The renormalized density of mobile species is found to be thermally activated up to 720 K with $E_a \sim 93$ meV, and above this temperature itinerant polarons move in an incoherent diffusive regime. The high spectral emissivity of this material that persists up to high temperatures and on a broad spectral domain is therefore related to diffusive carriers. More work is needed to check if it is possible to generalize such a concept to the high-temperature optical properties of doped transition metal oxides.

ACKNOWLEDGMENTS

B.R. thanks A.D.EM.E. (Agence de l'Environnement et De la Maîtrise de l'Energie) for financial support. The authors thank Dr. P. Simon (CRMHT Orléans), Dr. J. Dumas and Dr. S. Fratini (LEPES, Grenoble), Dr. R. P. S. M. Lobo (ESPCI Paris), Dr. A. Georges (LPT, Paris), Dr. J. Kreisel (LMGP, Grenoble), and Dr. J. M. Bassat and Professor M. Pouchard (ICMCB, Bordeaux) for helpful discussions.

[1] J. G. Bednorz and K. A. Müller, Z. Phys. B: Condens. Matter **64**, 189 (1986).
[2] S. Jin, T. H. Tiefel, M. MacCormack, R. A. Fastnacht, R. Ramesh, and L. H. Chen, Science, **264**, 413 (1994).
[3] C. H. Chen, S-W. Cheong, and A. S. Cooper, Phys. Rev. Lett. **71**, 2461 (1993).
[4] J. M. Tranquada, D. J. Buttrey, and V. Sachan, Phys. Rev. B **54**, 12318 (1996).
[5] J. M. Bassat, P. Odier, and F. Gervais, Phys. Rev. B **35**, 7126 (1987).
[6] L. Pintschovius, J. M. Bassat, P. Odier, F. Gervais, G. Chevrier, W. Reichardt, and F. Gompf, Phys. Rev. B **40**, 2229 (1989).
[7] T. Ido, K. Magoshi, H. Eisaki, and S. Uchida, Phys. Rev. B **44**, 12094 (1991).
[8] D. J. Buttrey, and J. M. Honig, in *Chemistry of High Temperature Superconductors*, edited by C. N. R. Rao (World Scientific, Singapore, 1992), pp. 283–305
[9] J. B. Goodenough, Mater. Res. Bull. **8**, 423 (1973).
[10] P. Ganguly and C. N. R. Rao, Mater. Res. Bull. **8**, 405 (1973).
[11] G. Demazeau, J. L. Marty, B. Buffat, J. M. Dance, M. Pouchard, P. Dordor, and B. Chevalier, Mater. Res. Bull. **17**, 37 (1982).
[12] G. Demazeau, J. L. Marty, M. Pouchard, T. Rojo, J. M. Dance, and P. Hagenmuller, Mater. Res. Bull. **16**, 47 (1981).
[13] C. N. R. Rao, D. J. Buttrey, N. Otsuka, P. Ganguly, H. R. Harisson, C. J. Sandberg, and J. M. Honig, J. Solid State Chem. **52**, 254 (1984).
[14] J. M. Bassat, P. Odier, and J. P. Loup, J. Solid State Chem. **110**, 124 (1994).
[15] V. V. Kharton, A. P. Viskup, E. N. Naumovich, and F. M. B. Marques, J. Mater. Chem. **9**, 2623 (1999).
[16] L. Minervi, R. W. Grimes, J. A. Kilner, and K. Sickafus, J. Mater. Chem. **10**, 2349 (2000).
[17] P. Odier, C. Allançon, and J. M. Bassat, J. Solid State Chem. **153**, 381 (2000).
[18] E. Boehm, J. M. Bassat, M. C. Steil, P. Dordor, F. Mauvy, and J. C. Grenier, Solid State Sci. **5**, 973 (2003).
[19] J. M. Bassat, P. Odier, A. Villesuzanne, C. Marin, and M. Pouchard, Solid State Ionics **167**, 341 (2004).

[20] M. Chabin, G. Duneau, D. De Sousa Meneses, P. Echegut, M. Malki, P. Odier, and B. Rousseau, European Patent No. 99,401,558.4-2214 (1999).
[21] B. Rousseau, A. Sin, P. Odier, F. Weiss, and P. Echegut, Appl. Phys. Lett. **79**, 3633 (2001).
[22] F. Gervais, R. P. S. M. Lobo, C. Allançon, N. Pellerin, J. M. Bassat, J. P. Loup, and P. Odier, Solid State Commun. **88**, 245 (1993).
[23] R. P. S. M. Lobo, C. Allançon, K. Dembinski, P. Odier, and F. Gervais, Solid State Commun. **88**, 349 (1993).
[24] D. M. Eagles, R. P. S. M. Lobo, and F. Gervais, Phys. Rev. B **52**, 6440 (1995).
[25] C. Allançon, A. Gonthier-Vassal, J. M. Bassat, J. P. Loup, and P. Odier, Solid State Ionics **74**, 239 (1994).
[26] C. Allançon, J. Rodriguez-Carvajal, M. T. Fernandez-Diaz, P. Odier, J. M. Bassat, J. P. Loup, and J. L. Martinez, Z. Phys. B: Condens. Matter **100**, 85 (1996).
[27] C. Allançon, P. Odier, J. M. Bassat, and J. P. Loup, J. Solid State Chem. **131**, 167 (1997).
[28] N. J. Poirot, C. Allançon, P. Odier, P. Simon, J. M. Bassat, and J. P. Loup, J. Solid State Chem. **138**, 260 (1998).
[29] M. T. Fernandez Diaz, J. L. Martinez, and J. Rodriguez-Carvajal, Solid State Ionics **63**, 902 (1993).
[30] X. X. Bi, P. C. Eklund, E. McRae, J. G. Zhuang, P. Metcalf, J. Spakek, and J. M. Honig, Phys. Rev. B **42**, 4756 (1990).
[31] X. X. Bi, P. C. Eklund, and J. M. Honig, Phys. Rev. B **48**, 3470 (1993).
[32] D. A. Crandles, T. Timusk, J. D. Garret, and J. E. Greedan, Physica C **216**, 94 (1993).
[33] P. Calvani, A. Paolone, P. Dore, S. Lupi, P. Maselli, P. G. Medaglia, and S. W. Cheung, Phys. Rev. B **54**, R9592 (1996).
[34] T. Katsufuji, T. Tanabe, T. Ishikawa, Y. Fukuda, T. Arima, and Y. Tokura, Phys. Rev. B **54**, R14230 (1996).
[35] N. Poirot-Reveau, P. Odier, P. Simon, and F. Gervais, Phys. Rev. B **65**, 094503 (2002).
[36] F. Gervais, Mater. Sci. Eng., R. **39**, 22 (2002).
[37] C. C. Homes, J. M. Tranquada, Q. Li, A. R. Moodenbaugh, and D. J. Buttrey, Phys. Rev. B **67**, 184516 (2003).
[38] B. Rousseau, J. M. Bassat, A. Blin, M. S de Oliveira, P. Odier, C. Marin, P. Simon, Solid State Sci. **6**, 1131 (2004).
[39] J. Oreinstein, G. A. Thomas, D. H. Rapkine, C. G. Bethea, B. F. Levine, B. Batlog, R. J. Cava, D. W. Johnson, and E. A. Rietman, Phys. Rev. B **36**, 8892 (1987).
[40] F. Gervais, P. Echegut, J. M. Bassat, and P. Odier, Phys. Rev. B **37**, 9364 (1988).
[41] S. Uchida, H. Ido, H. Takagi, T. Arima, Y. Tokura, and S. Tajima, Phys. Rev. B **43**, 7942 (1991).
[42] J .P. Falck, A. Levy, M. A. Kastner, and R. J. Birgeneau, Phys. Rev. B **48**, 4043 (1993).
[43] P. Calvani, M. Capizzi, S. Lupi, P. Maselli, A. Paolone, and P. Roy, Phys. Rev. B **53**, 2756 (1996).
[44] F. Gervais, R. P. S. M. Lobo, M. Licheron, and F. J. Gotor, Ferroelectrics **177**, 107 (1996).
[45] S. Pessaud and F. Gervais, Mater. Sci. Eng., B **86**, 200 (2001).
[46] K. Takenaka, J. Nohara, R. Shiozaki, and S. Sugai, Phys. Rev. B **68**, 134501 (2003).
[47] A. EL Azrak, R. Nahoon, A. C. Baccarra, N. Bontemps, M. Guilloux-Viry, C. Thiret, A. Perrin, Z. Z. Li, and H. Raffy, J. Alloys Compd. **19**, 663 (1993).
[48] P. W. Anderson, Phys. Rev. **109**, 1492 (1958).
[49] K. Dembinski, J. M. Bassat, J. P. Coutures, and P. Odier, J. Mater. Sci. Lett. **6**, 1365 (1987).
[50] F. Gervais, in *Infrared and Millimeter Wave*, edited by K. J. Button (Academic, New York, 1983), vol. 8, p. 279.
[51] N. Petit, C. Daulan, J-C. Soret, A. Maignan, and F. Gervais, Eur. Phys. J. B **14**, 617 (2000).
[52] T. Kurosawa, J. Phys. Soc. Jpn. **16**, 1298 (1961).
[53] E. Shiles, T. Sasaki, M. Inokuti, and D. Y. Smith, Phys. Rev. B **22**, 1612 (1980).
[54] J. F. Brun, D. De Sousa Meneses, B. Rousseau, and P. Echegut, Appl. Spectrosc. **55**, 774 (2001).
[55] N. E. Massa, H. Falcon, H. Salva, and R. E. Carbonio, Phys. Rev. B **56**, 10178 (1997).
[56] C. Allançon, Ph.D. thesis, the University of Orleans, 1995.
[57] N. F. Mott, *Metal-Insulator Transitions* (Taylor & Francis, London, 1990), p. 59.
[58] R. S. P. M. Lobo, E. Y. Sherman, D. Racah, Y. Dagan, and N. Bontemps, Phys. Rev. B **65**, 104509 (2002).
[59] G. I. Bersuker and J. B. Goodenough, Physica C **274**, 267 (1997).
[60] D. Emin, Phys. Rev. B **48**, 13691 (1993).
[61] G. Iadonisi, V. Cataudella, and G. De Filippis, Physica B **265**, 146 (1999).
[62] K. A. Muller, G. M. Zhao, K. Conder, and H. Keller, J. Phys.: Condens. Matter **10**, 291 (1998).
[63] J. B. Goodenough, J. Less-Common Met. **116**, 83 (1986).